

Hierarchical cycle-tree packing model for K -core attack problem

Jianwen Zhou^{1,2} and Hai-Jun Zhou^{1,2,3*}

¹CAS Key Laboratory for Theoretical Physics, Institute of Theoretical Physics, Chinese Academy of Sciences, Beijing, 100190, China.

²School of Physical Sciences, University of Chinese Academy of Sciences, Beijing, 100049, China.

³MinJiang Innovative Center for Theoretical Physics, MinJiang University, Fuzhou, 350108, China.

*Corresponding author(s). E-mail(s): zhouhj@itp.ac.cn;

Abstract

The K -core of a graph is the unique maximum subgraph within which each vertex connects to at least K other vertices. The K -core optimal attack problem asks to construct a minimum-sized set of vertices whose removal results in the complete collapse of the K -core. In this paper, we construct a hierarchical cycle-tree packing model which converts a long-range correlated K -core pruning process into static patterns and analyze this model through the replica-symmetric (RS) cavity method of statistical physics. The cycle-tree guided attack (CTGA) message-passing algorithm exhibits superior performance on random regular and Erdős–Rényi graphs. It provides new upper bounds on the minimal cardinality of the K -core attack set. The model of this work may be extended to construct optimal initial conditions for other irreversible dynamical processes.

Keywords: K -core, cavity method, message-passing algorithm

1 Introduction

The concept of K -core was introduced to study the magnetization in lattices [1] and the collective behaviors in social networks [2, 3]. The K -core of a graph is

the maximum induced subgraph such that each vertex connects to at least K other vertices. This subgraph can be obtained by recursively deleting vertices whose degrees are less than K .

K -core can capture some of the key properties of many networks and has a wide range of applications [4]. In biology, the K -cores of protein-protein interaction networks along with phylogenetic analysis has been used to predict the function of certain function-unknown proteins [5], and the innermost K -cores are prolific, essential, and evolutionary conserved which might constitute a putative evolutionary backbone of the proteome [6]. K -core percolation is used to study the conscious to subliminal transition in the brain [7]. K -shell decomposition in the brain network suggests that K -core structure might help protect against cognitive decline in aging [8]. In ecology, the K -core decomposition is utilized to understand the robustness of bipartite mutualistic networks and helps to identify key species to preserve [9]. In social networks, the K -core decomposition shows that the most efficient spreaders are those located within the most densely connected K -core (whose value of K is the maximum) [10], which can be used to analyze the spread of disease, information, and rumor. Since K -core structure plays important roles in numerous domains, it would be of great interest to perform efficient adversarial attacks or protect as few nodes as possible to enhance its robustness.

In this paper, we consider a graph $G = (V, E)$ consisting of $N = |V|$ vertices and $M = |E|$ undirected edges. The vertices in the vertex set V are indexed by positive integers i, j, k, \dots , and the set E of undirected edges contains pairs of neighboring vertices. An edge between two vertices i and j is denoted by (i, j) . The neighborhood of vertex i is the set $\partial i \equiv \{j : (i, j) \in G\}$ which contains all the nearest neighbors of vertex i , and the cardinality of this set is called the degree d_i of vertex i .

In the threshold model [2] or the bootstrapping percolation [11] in physics, the vertices in graph G can be either active or inactive, and active vertices will remain active for the rest of the process. In the percolation process, once the number of active neighbors of an inactive vertex i reaches a threshold t_i , vertex i will become active. One can define an optimal initial condition problem as follows: find the minimal number of initially active vertices such that eventually the entire graph is active. It is known as the minimal contagious set problem [12–14] or the smallest irreversible K -conversion set [15]. We can also consider this optimization problem from an alternative way: The K -core optimal attack problem is to find the minimum set of vertices such that the removal of those vertices leads to an empty K -core. It is similar to the collapsed K -core problem [16] which aims to find a given number of vertices so that after removing these vertices, we obtain the smallest k -core. The conversion relation between the threshold t_i in the minimal contagious set problem and the value of K in the K -core attack problem is that $t_i = d_i - K + 1$ where d_i is the degree of vertex i . This optimization problem in general graphs is known to be NP-hard [15].

The standard theoretical framework maps the irreversible threshold dynamics into a static Potts model with $T + 1$ states $t_i \in \{0, 1, \dots, T\}$, where $t_i = 0$ means that vertex i is the seed of dynamics, and $t_i \geq 1$ means that vertex i is affected (or removed) at the t_i -th time step following the dynamical evolution rule [14, 17–21]. Under this framework, the minimal contagious set problem has been thoroughly studied using the cavity method on random regular graphs, and a survey-propagation-like algorithm was proposed to find the minimal contagious set [14].

For the special case of $K = 2$, this problem is known as the minimum feedback vertex set (FVS) problem (or decycling problem) which aims to destroy all the cycles in the graph and it is one of the classic NP-complete problems [22]. The rigorous upper and lower bounds of the decycling number for random regular graphs are given in [23]. The belief propagation-guided decimation (BPD) algorithm [20, 24] and Min-Sum algorithm [19] inspired by statistical physics are well performed on this optimization problem.

For general K , CoreHD [25] is a simple and effective sub-optimal method that iteratively removes one of the vertices with the highest degree in the remaining K -core. The performance of CoreHD is further improved by the WEAK-NEIGHBOR (WN) algorithm [26], which iteratively removes one of the nodes with high degree and low average degree of the neighbors. Remarkably, the WN algorithm outperforms the message-passing CI-TM algorithm [27] which measures the significance of spreaders in global cascades by the number of subcritical paths as well as other scalable algorithms [17, 18]. For the case of K -core attack problem with $K \geq 3$, there are still non-negligible gaps between the best known algorithmic upper bounds[26] and the expected exact theoretical predictions[14].

To efficiently find a better solution to this problem, we propose a Hierarchical cycle-tree packing model which reformulates the irreversible K -core pruning dynamics in a form of statistical mechanics that can be treated with the cavity method.[28, 29]. This model is inspired by the spin glass model for the FVS problem [24] and is an expansion to the cycle-tree packing model [30]. We demonstrate that by allowing different (cycle-)tree components to be distributed in at most H layers the (cycle-)tree packing model can better characterize the K -core pruning process with less states of the spin glass model. The inspired message-passing algorithm outperforms the state-of-the-art algorithm [26] on random regular and Erdős–Rényi graphs and could be further improved by expanding the number of layers. Our reformulation of an irreversible dynamical process into static structural patterns may be instructive to other hard optimization problems.

The paper is organized as follows. In Section 2, we introduce the hierarchical cycle-tree packing model for the K -core attack problem. In Section 3, we analyze this model by replica symmetric (RS) cavity method of statistical physics and derive the belief propagation equation. In section 4.1, we present the theoretical results of random regular graphs. In Section 4.2, we

4 Hierarchical cycle-tree packing model for K -core attack problem

propose a heuristic algorithm and show its performance on random regular and Erdős–Rényi graphs.

2 Model

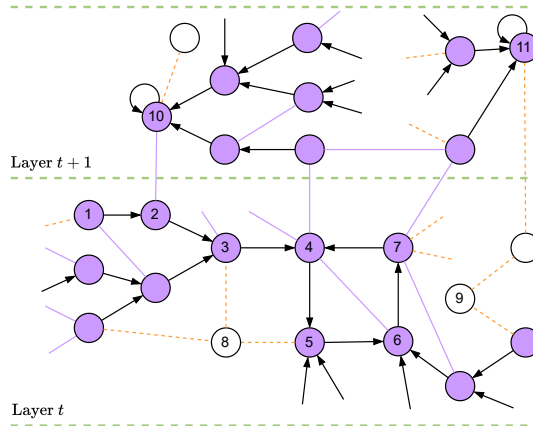


Fig. 1 Part of the hierarchical cycle-trees, showing one cycle-tree in a lower layer and two directed trees in a higher layer. The colored circles represent occupied vertices and the uncolored circles represent empty vertices. Edges between occupied vertices are drawn as solid lines, and edges between empty vertices and others are drawn as dashed lines. An arrow-decorated solid edges in layer t , e.g., $3 \rightarrow 4$, indicates the state of vertex 3 being $A_3 = 4^t$. A root vertex, e.g., vertex 10, has a self-pointed edge, and its state is $A_{10} = 10^{t+1}$. Each occupied vertex has exactly one out-going edge and the number of arrow-free solid edges is restricted.

We represent the K -core pruning process by static and hierarchical directed trees and cycle-trees (Figure 1). A cycle-tree [24] is referred to as a directed cycle plus a set of directed tree branches pointing to this cycle. To represent this model, we assign arrows to certain edges of the graph.

In this model, each (cycle-)tree can be regarded as the basic unit of k -kernel pruning, and they are allocated in a total of H layers. In the k -core pruning process, the vertices of the attack set will be removed first, and then starting from the first layer, the cycle-trees of each layer will be removed layer by layer because they can not sustain the K -core until the H -th layer.

To describe the local constraint of this model, we begin with assigning a discrete state $A_i \in \{0\} \cup \{i^t : t = 1, 2, \dots, H\} \cup \{j^t : j \in \partial i, t = 1, 2, \dots, H\}$ to each vertex i of the graph G . There are $H(d_i + 1) + 1$ distinct possible states for each vertex. The constraint on vertex i and its neighbors ∂i can be written

in the following trivial form

$$C_i(A_i, \underline{A}_{\partial i}) = \delta_{A_i}^0 C_i(0, \underline{A}_{\partial i}) + \sum_{t=1}^H \delta_{A_i}^{i^t} C_i(i^t, \underline{A}_{\partial i}) + \sum_{t=1}^H \sum_{j \in \partial i} \delta_{A_i}^{j^t} C_i(j^t, \underline{A}_{\partial i}), \quad (1)$$

where $\underline{A}_{\partial i} \equiv \{A_j; j \in \partial i\}$ contains the states of the neighbors of vertex i , $\delta_m^n = 1$ if $n = m$ otherwise $\delta_m^n = 0$. If the constraint of vertex i is met, we have $C_i(A_i, \underline{A}_{\partial i}) = 1$ and $= 0$ otherwise. Vertex i is said to be empty if $A_i = 0$ and it will be removed before the K -core pruning process; otherwise it is said to be occupied. An empty vertex neither points to any vertices nor is pointed to by any vertices. The edges between an empty vertex and its neighbors are represented by arrow-free dashed edges. Every occupied vertex has exactly one outgoing edge that points to either its neighbor vertices located at the same layer or to itself. But the number of edges that point to the same vertex is unrestricted. Note that the edges between vertices of different layers must be arrow-free. More specifically, if $A_i = i^t$ for $t = 1, 2, \dots, H$, we call it a root at t which means that it points to itself and is located at layer t . A root can not point to its neighbors due to the constraints so it can only point to itself. If $A_i = j^t$ for $j \in \partial i$ and $t = 1, 2, \dots, H$, it means that vertex i points to vertex j at the same layer t and vertex j shall be occupied but not pointing to i .

Each vertex i must satisfy the following local constraint: (1) if vertex i is empty ($A_i = 0$), its neighbors could be in any state, i.e.,

$$C_i(0, \underline{A}_{\partial i}) = \prod_{j \in \partial i} \left(\delta_{A_j}^0 + \sum_{t=1}^H \delta_{A_j}^{j^t} + \sum_{t=1}^H \sum_{l \in \partial j \setminus i} \delta_{A_j}^{l^t} \right), \quad (2)$$

where the set $\partial i \setminus j$ contains all the nearest neighbors of vertex i excluding j . (2) If vertex i is a root at layer $t = 1$ ($A_i = i^1$), then the total number of vertices that are roots or point to their neighbor except for vertex i at layer $t' \geq 2$ shall be at most $K - 1$:

$$C_i(i^1, \underline{A}_{\partial i}) = \prod_{j \in \partial i} \left[\delta_{A_j}^0 + \delta_{A_j}^{i^1} + \sum_{t=2}^H \left(\delta_{A_j}^{j^t} + \sum_{l \in \partial j \setminus i} \delta_{A_j}^{l^t} \right) \right] \times \Theta \left[K - 1 - \sum_{j \in \partial i} \sum_{t=2}^H \left(\delta_{A_j}^{j^t} + \sum_{l \in \partial j \setminus i} \delta_{A_j}^{l^t} \right) \right], \quad (3)$$

where the step function $\Theta(x) = 1$ if $x \geq 0$ otherwise $\Theta(x) = 0$. (3) If vertex i points to j at layer $t = 1$ ($A_i = j^1$), then the total number of its neighbors except for j which point to their neighbors except for i at layer $t = 1$ or are

occupied at higher layer $t \geq 2$ shall be at most $K - 2$, i.e.,

$$\begin{aligned}
 C_i(j^1, \underline{A}_{\partial i}) &= \left(\delta_{A_j}^{j^1} + \sum_{l \in \partial j \setminus i} \delta_{A_j}^{l^1} \right) \\
 &\times \prod_{k \in \partial i \setminus j} \left[\delta_{A_k}^0 + \delta_{A_k}^{i^1} + \sum_{l \in \partial k \setminus i} \delta_{A_k}^{l^1} + \sum_{t=2}^T \left(\delta_{A_k}^{k^t} + \sum_{l \in \partial k \setminus i} \delta_{A_k}^{l^t} \right) \right] \\
 &\times \Theta \left\{ K - 2 - \sum_{k \in \partial i \setminus j} \left[\sum_{l \in \partial k \setminus i} \delta_{A_k}^{l^1} + \sum_{t=2}^H \left(\delta_{A_k}^{k^t} + \sum_{l \in \partial k \setminus i} \delta_{A_k}^{l^t} \right) \right] \right\}. \tag{4}
 \end{aligned}$$

(4) If vertex i is a root at layer $t \geq 2$, then the total number of vertices that point to their neighbors except i at layer $t - 1$, point to i at layer t , or are occupied at higher layer $t' \geq t + 1$ shall be at least K , while the total number of vertices which are occupied at higher layer $t' \geq t + 1$ shall be at most $K - 1$. Thus for $2 \leq t \leq H$, we have

$$\begin{aligned}
 C_i(i^t, \underline{A}_{\partial i}) &= \\
 &\prod_{j \in \partial i} \left[\delta_{A_j}^0 + \sum_{s=1}^{t-1} \left(\delta_{A_j}^{j^s} + \sum_{l \in \partial j \setminus i} \delta_{A_j}^{l^s} \right) + \delta_{A_j}^{i^t} + \sum_{s=t+1}^H \left(\delta_{A_j}^{j^s} + \sum_{l \in \partial j \setminus i} \delta_{A_j}^{l^s} \right) \right] \\
 &\times \Theta \left\{ \sum_{j \in \partial i} \left[\sum_{l \in \partial j \setminus i} \delta_{A_j}^{l^{t-1}} + \delta_{A_j}^{i^t} + \sum_{s=t+1}^H \left(\delta_{A_j}^{j^s} + \sum_{l \in \partial j \setminus i} \delta_{A_j}^{l^s} \right) \right] - K \right\} \tag{5} \\
 &\times \Theta \left[K - 1 - \sum_{j \in \partial i} \sum_{s=t+1}^H \left(\delta_{A_j}^{j^s} + \sum_{l \in \partial j \setminus i} \delta_{A_j}^{l^s} \right) \right].
 \end{aligned}$$

(5) If vertex i points to j at layer $t \geq 2$ ($A_i = j^t$), then the total number of its neighbors except for j which point to their neighbor except for i at layer $t - 1$ or are occupied at layer $t' \geq t$ shall be at least $K - 1$, while the total number of its neighbors except for j which point to their neighbor except for i at layer t or are occupied at layer $t' \geq t + 1$ shall be at most $K - 2$. Thus for

$2 \leq t \leq H$, we have

$$\begin{aligned}
 C_i(j^t, \underline{A}_{\partial i}) &= \left(\delta_{A_j}^{j^t} + \sum_{l \in \partial j \setminus i} \delta_{A_j}^{l^t} \right) \\
 &\times \prod_{k \in \partial i \setminus j} \left(\delta_{A_k}^0 + \sum_{s=1}^{t-1} \delta_{A_k}^{k^s} + \sum_{s=1}^{t-2} \sum_{l \in \partial k \setminus i} \delta_{A_k}^{l^s} + \delta_{A_k}^{i^t} + \sum_{l \in \partial k \setminus i} \delta_{A_k}^{l^{t-1}} \right. \\
 &\quad \left. + \sum_{s=t+1}^H \delta_{A_k}^{k^s} + \sum_{s=t}^H \sum_{l \in \partial k \setminus i} \delta_{A_k}^{l^s} \right) \tag{6} \\
 &\times \Theta \left[\sum_{k \in \partial i \setminus j} \left(\delta_{A_k}^{i^t} + \sum_{l \in \partial k \setminus i} \delta_{A_k}^{l^{t-1}} + \sum_{s=t+1}^H \delta_{A_k}^{k^s} + \sum_{s=t}^H \sum_{l \in \partial k \setminus i} \delta_{A_k}^{l^s} \right) - K + 1 \right] \\
 &\times \Theta \left[K - 2 - \sum_{k \in \partial i \setminus j} \left(\sum_{s=t+1}^H \delta_{A_k}^{k^s} + \sum_{s=t}^H \sum_{l \in \partial k \setminus i} \delta_{A_k}^{l^s} \right) \right].
 \end{aligned}$$

When the constraints of this model are satisfied, the occupied vertices connected by arrow-decorated edges form a set of directed trees and cycle-trees. There could be arrow-free solid edges between vertices of the same (cycle-)tree or between two different (cycle-)trees. If all the empty vertices are removed from graph G , the (cycle-)trees at the first layer can not sustain a K -core and will collapse from the leaf vertices at the first layer and propagate to the root vertices or the directed cycles (one of their vertices needs to be removed manually to eliminate the cycle-trees). After the collapse of the (cycle-)trees at the first layer, in the same way, the (cycle-)trees at the second layer can not sustain a K -core. The collapse will persist hierarchically until the last layer. Thus the empty vertices from a K -core attack set.

If $H = 1$, this model is reduced to the model of Ref. [30]. Furthermore, if $K = 2$, this model is identical to the feedback vertex set model of Ref. [24] (and the layer number H becomes irrelevant). Since for $K = 2$, after the removal of empty vertices, in our model, the undirected edge could only exist between cross-layer root vertices, and those connected root vertices could only form trees due to the constraint. If we assign those undirected edges with arrows from the lower layer to the higher layer, the connected cycle-trees are combined into a single cycle-tree. Thus, for the cases of $k = 2$, generalization to hierarchical models is not necessary but increases the complexity of the calculation.

We then introduce an energy function $E(\underline{A}) = \sum_i \delta_{A_i}^0$ to give different probabilistic weights to different attack sets that are subject to the constraints (1) for all links, $p(\underline{A}) \propto \exp[-\beta E(\underline{A})]$, where $\delta_{A_i}^0$ is the ‘cost’ incurred by adding vertex i into the attack set. To encourage a minimal attack set for this optimal problem, we impose a penalty factor $e^{-\beta}$ with inverse temperature β to each empty vertex. When β is large, the distribution will be concentrated

on certain attack sets that are much smaller than the average. When $\beta \rightarrow \infty$, only the smallest attack set is selected. The selection of a larger H means loosening the constraint and leads to lower energy. Thus, the partition function of the spin glass model is

$$Z(\beta) = \sum_{\underline{A}} \prod_{i=1}^N \left[e^{-\beta \delta_{A_i}^0} C_i(A_i, \underline{A}_{\partial i}) \right],$$

where $\underline{A} = \{A_1, \dots, A_N\}$ is the configuration of the system, and $\sum_{\underline{A}}$ means summing over all possible configurations of N vertices. The joint probability distribution of the states of N vertices is expressed as

$$q(\underline{A}) = \frac{1}{Z(\beta)} \prod_{i=1}^N \left[e^{-\beta \delta_{A_i}^0} C_i(A_i, \underline{A}_{\partial i}) \right]. \quad (7)$$

3 The belief propagation equations

We adopt the standard cavity method of statistical physics [28, 29] to estimate the marginal probability q_i^0 of vertex i being empty (details are shown in Appendix 7.1). For every directed edge (i, j) we denote by $q_{i \rightarrow j}(A_i, A_j)$ the cavity marginal probability (or belief) of states A_i and A_j . A self-consistent belief-propagation (BP) equation for all $q_{i \rightarrow j}(A_i, A_j)$ s can be easily derived. By noting that the values of $q_{i \rightarrow j}(A_i, A_j)$ for certain A_i and A_j are identical and certain $q_{i \rightarrow j}(A_i, A_j)$ s always appear under the form of particular linear combinations, we can parameterize the cavity marginal probability and obtain the more compact form of the BP equation, i.e.,

$$Q_{i \rightarrow j}^0 \propto e^{-\beta} \prod_{k \in \partial i \setminus j} \left(Q_{k \rightarrow i}^0 + \sum_{t=1}^H Q_{k \rightarrow i}^{1,t} \right); \quad (8a)$$

$$Q_{i \rightarrow j}^{1,1} \propto G_1(K-1, \partial i \setminus j) + \sum_{k' \in \partial i \setminus j} Q_{k' \rightarrow i}^{1,1} G_2(K-2, \partial i \setminus j \setminus k'); \quad (8b)$$

$$Q_{i \rightarrow j}^{3,1} \propto G_1(K-2, \partial i \setminus j); \quad (8c)$$

$$Q_{i \rightarrow j}^{4,1} \propto G_2(K-2, \partial i \setminus j); \quad (8d)$$

$$Q_{i \rightarrow j}^{5,1} \propto \sum_{k' \in \partial i \setminus j} Q_{k' \rightarrow i}^{1,1} G_2(K-3, \partial i \setminus j \setminus k'); \quad (8e)$$

$$Q_{i \rightarrow j}^{1,t} \propto \sum_{k' \in \partial i \setminus j} Q_{k' \rightarrow i}^{2,t} G_4^t(K-2, K-1, \partial i \setminus j \setminus k') + G_3^t(K-1, K, \partial i \setminus j), \quad 2 \leq t \leq H; \quad (8f)$$

$$Q_{i \rightarrow j}^{2,t} \propto \sum_{k' \in \partial i \setminus j} Q_{k' \rightarrow i}^{2,t} G_4^t(K-2, K-2, \partial i \setminus j \setminus k') + G_3^t(K-1, K-1, \partial i \setminus j), \quad 2 \leq t \leq H; \quad (8g)$$

$$Q_{i \rightarrow j}^{3,t} \propto G_3^t(K-2, K-1, \partial i \setminus j), \quad 2 \leq t \leq H-1; \quad (8h)$$

$$Q_{i \rightarrow j}^{4,t} \propto G_4^t(K-2, K-1, \partial i \setminus j), \quad 2 \leq t \leq H; \quad (8i)$$

$$Q_{i \rightarrow j}^{5,t} \propto \sum_{k' \in \partial i \setminus j} Q_{k' \rightarrow i}^{2,t} G_4^t(K-3, K-2, \partial i \setminus j \setminus k'), \quad 2 \leq t \leq H, \quad (8j)$$

where the \propto symbol contains a multiplicative normalization constant and we define

$$G_1(x, S) = \sum_{\substack{|I| \leq x \\ I \cup J = S}} \prod_{k \in I} \left(\sum_{t=2}^H Q_{k \rightarrow i}^{1,t} \right) \prod_{n \in J} \left(Q_{n \rightarrow i}^0 + Q_{n \rightarrow i}^{4,1} \right); \quad (9a)$$

$$G_2(x, S) = \sum_{\substack{|I| \leq x \\ I \cup J = S}} \prod_{k \in I} \left(Q_{k \rightarrow i}^{5,1} + Q_{k \rightarrow i}^{2,2} + \sum_{t=3}^H Q_{k \rightarrow i}^{1,t} \right) \prod_{n \in J} \left(Q_{n \rightarrow i}^0 + Q_{n \rightarrow i}^{4,1} \right); \quad (9b)$$

$$G_3^t(x, y, S) = \sum_{\substack{|I| \leq x \\ |I| + |J| \geq y \\ I \cup J \cup L = S}} \prod_{k \in I} \left(\sum_{s=t+1}^H Q_{k \rightarrow i}^{1,s} \right) \prod_{n \in J} \left(Q_{n \rightarrow i}^{5,t-1} + Q_{n \rightarrow i}^{4,t} \right) \quad (9c)$$

$$\begin{aligned} & \times \prod_{m \in L} \left(Q_{m \rightarrow i}^0 + \sum_{s=1}^{t-1} Q_{m \rightarrow i}^{3,s} + \sum_{s=1}^{t-2} Q_{m \rightarrow i}^{5,s} \right); \\ G_4^t(x, y, S) &= \sum_{\substack{|I| \leq x \\ |I| + |J| \geq y \\ I \cup J \cup L = S}} \prod_{k \in I} \left(Q_{k \rightarrow i}^{2,t+1} + \sum_{s=t+2}^H Q_{k \rightarrow i}^{1,s} + Q_{k \rightarrow i}^{5,t} \right) \\ & \times \prod_{n \in J} \left(Q_{n \rightarrow i}^{5,t-1} + Q_{n \rightarrow i}^{4,t} \right) \prod_{m \in L} \left(Q_{m \rightarrow i}^0 + \sum_{s=1}^{t-1} Q_{m \rightarrow i}^{3,s} + \sum_{s=1}^{t-2} Q_{m \rightarrow i}^{5,s} \right). \end{aligned} \quad (9d)$$

Please note that the symbols $G(\dots)$ above are related to $\{Q_{k \rightarrow i}^{\dots}\}_{k \in S}$ but we omit them for the sake of brevity. The summation $\sum_{\substack{|I| \leq x \\ I \cup J = S}}$ is over the

partitions I, J of S with the constraint that the cardinality of the set I is less than or equal to x . There are $5H - 1$ distinct cavity probabilities in the BP

equation for each directed edge. The normalization condition is given by

$$(1 + d_j H)Q_{i \rightarrow j}^0 + \sum_{t=1}^{H-1} (H-t)d_j Q_{i \rightarrow j}^{3,t} + \sum_{t=2}^H \left[((t-2)d_j + 2)Q_{i \rightarrow j}^{1,t} + d_j Q_{i \rightarrow j}^{2,t} \right] + \sum_{t=1}^H \left[d_j Q_{i \rightarrow j}^{4,t} + ((H-t+1)d_j - 1)Q_{i \rightarrow j}^{5,t} \right] + 2Q_{i \rightarrow j}^{1,1} = 1. \quad (10)$$

After obtaining the fixed point solution of the BP Equation (8), the free energy density is computed by

$$f = -\frac{1}{\beta N} \sum_i \ln z_i + \frac{1}{\beta N} \sum_{(i,j) \in E} \ln z_{ij}, \quad (11)$$

where $\sum_{(i,j) \in E}$ runs over the undirected edges of the graph. The local partition functions are computed by

$$\begin{aligned} z_{ij} = & Q_{i \rightarrow j}^0 Q_{j \rightarrow i}^0 + Q_{i \rightarrow j}^{1,1} Q_{j \rightarrow i}^{4,1} + Q_{i \rightarrow j}^{4,1} Q_{j \rightarrow i}^{1,1} + \sum_{t=1}^H \left(Q_{i \rightarrow j}^{1,t} Q_{j \rightarrow i}^0 + Q_{i \rightarrow j}^0 Q_{j \rightarrow i}^{1,t} \right) \\ & + \sum_{t=2}^H \left(Q_{i \rightarrow j}^{4,t} Q_{j \rightarrow i}^{2,t} + Q_{i \rightarrow j}^{2,t} Q_{j \rightarrow i}^{4,t} \right) + \sum_{t=2}^H \sum_{s=1}^{t-1} \left(Q_{i \rightarrow j}^{3,s} Q_{j \rightarrow i}^{1,t} + Q_{i \rightarrow j}^{1,t} Q_{j \rightarrow i}^{3,s} \right) \\ & + \sum_{t=3}^H \sum_{s=1}^{t-2} \left(Q_{i \rightarrow j}^{1,t} Q_{j \rightarrow i}^{5,s} + Q_{i \rightarrow j}^{5,s} Q_{j \rightarrow i}^{1,t} \right) + \sum_{t=1}^{H-1} \left(Q_{i \rightarrow j}^{2,t+1} Q_{j \rightarrow i}^{5,t} + Q_{i \rightarrow j}^{5,t} Q_{j \rightarrow i}^{2,t+1} \right) \\ & + \sum_{t=1}^H Q_{i \rightarrow j}^{5,t} Q_{j \rightarrow i}^{5,t}, \end{aligned} \quad (12)$$

and

$$\begin{aligned} z_i = & e^{-\beta} \prod_{k \in \partial i} \left(Q_{k \rightarrow i}^0 + \sum_{t=1}^H Q_{k \rightarrow i}^{1,t} \right) + G_1(K-1, \partial i) \\ & + \sum_{k' \in \partial i} Q_{k' \rightarrow i}^{1,1} G_2(K-2, \partial i \setminus k') + \sum_{t=2}^H G_3^t(K-1, K, \partial i) \\ & + \sum_{t=2}^H \sum_{k' \in \partial i} Q_{k' \rightarrow i}^{2,t} G_4^t(K-2, K-1, \partial i \setminus k'). \end{aligned} \quad (13)$$

The probability that vertex i is empty is then reduced to

$$q_i^0 = \frac{1}{z_i} e^{-\beta} \prod_{k \in \partial i} \left(Q_{k \rightarrow i}^0 + \sum_{t=1}^H Q_{k \rightarrow i}^{1,t} \right). \quad (14)$$

Thus the energy density ρ is defined by the mean fraction of empty vertices (or the mean fraction of vertices in the attack set):

$$\rho = \frac{1}{N} \sum_{i=1}^N q_i^0. \quad (15)$$

Finally, the entropy density is simply $s = \beta(\rho - f)$.

4 Results

4.1 Mean-field results in random regular graph

We calculate the theoretical prediction in random regular (RR) networks for which the belief propagation equations are much simplified since all messages $Q_{i \rightarrow j}^\sigma$ are the same for all directed edges (i, j) in the thermodynamic limit $N \rightarrow \infty$. The technical detail is given in Appendix 7.2. To obtain the numerical solution, we need to solve a set of $5H - 1$ equations on $5H - 1$ unknowns by Newton-Raphson iterative method with proper choice of the initial condition.

The numerical results for $D = 7$ and $K = 3$ are shown in Figure 2. The qualitative features are independent of D and K . As shown in Figure 2(a), the energy density should decrease as β increases, and reach a finite limit when $\beta \rightarrow \infty$, that would be the ground state energy density of the system if the RS cavity theory is correct in this limit. However, it's not true because the entropy will become negative as β increases, as shown in Figure 2(b), which indicates that the RS cavity theory becomes inadequate in this regime. Thus, the energy density at the point of entropy vanishment would be the best guess from the RS cavity theory and it's defined as by the ground state energy. In Figure 2(c), we display the results of entropy density s as the function of energy density ρ for various values of H . It could be presumed that for $K \geq 3$ as H increases, the ground state energy density decreases and converge to a limit as $H \rightarrow \infty$. As we have discussed above, for $K = 2$, the curves of entropy and energy density for any values of H will coincide.

In Figure 2(d), we compare the ground state energy density obtained by our model with that by the RS cavity method of [14] under various values of the time level H (or T). It's worth noting that in our model, the cavity probability of each directed edge has $5H - 1$ values, while it's $2T$ in the RS cavity method of [14]. As $T \rightarrow \infty$, the ground state energy density obtained by the RS cavity method of [14] will converge to about 0.3000897, while that obtained by our model would be slightly smaller than the former (the ground state energy density of our model when $H = 16$ is 0.3000870). Moreover, as shown in Table 1, for $K = 2$ and $D \geq 5$, the ground state energy densities obtained by our model (which are independent of the values of H) are slightly smaller than that obtained by [14]. This is because there are few nodes (the quantity is equal to the number of cycle-trees) that need to be removed manually in the cycle-tree packing model and they are not counted in the energy. Nevertheless, even for

a low time level, our model predicts a much lower ground state energy density, which may guide us to develop much more efficient algorithms for optimizing the K -core attack set problem.

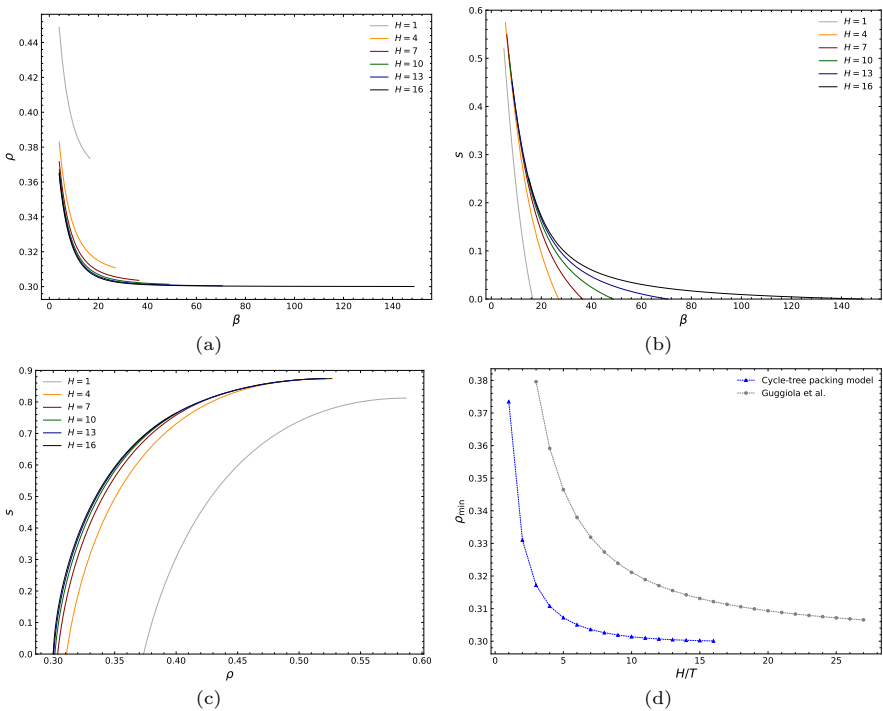


Fig. 2 Theoretical predictions for the random regular graph of degree $D = 7$ and the K -core threshold $K = 3$ with different H s. (a) Energy density ρ vs. inverse temperature β , computed from the replica symmetric cavity equations. We only display the curves in the regime of $s \geq 0$. (b) Entropy density s vs. inverse temperature β . (c) Energy density ρ vs. entropy density s . (d) Ground state energy density ρ_{\min} vs. the value of H (or T). As a comparison, the gray points are the results obtained via the RS cavity method in [14].

Algorithm 1 Cycle-Tree-Guided-Attack algorithm

-
- 1: initialize BP messages
 - 2: initialize the attack set $\Gamma = \emptyset$
 - 3: initialize graph G with vertex set V
 - 4: **while** $V \neq \emptyset$ **do**
 - 5: iterate BP equations for certain repeats
 - 6: calculate the BP marginal $\{q_i^0; i \in V\}$
 - 7: choose vertex $i = \arg \max_j q_j^0$
 - 8: **if** $\text{rand}() < q_i^0$ **then**
 - 9: set $\Gamma \leftarrow \Gamma \cup \{i\}$
 - 10: set $V \leftarrow V \setminus i$
 - 11: $G \leftarrow K\text{-core}(G)$
 - 12: **end if**
 - 13: **end while**
 - 14: **return** the attack set Γ
-

4.2 The results of cycle-tree guided attack algorithm

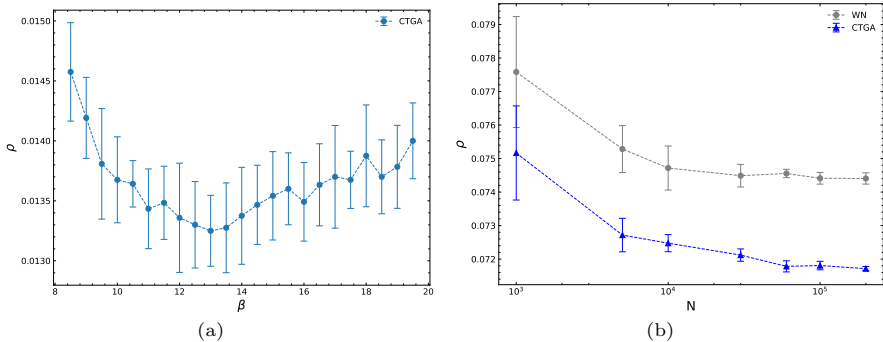


Fig. 3 (a) The performance of CTGA algorithm of $H = 3$ on random regular graphs with $D = 6, K = 5$, and different values of β . The algorithmic results are averaged over 12 instances of random regular graphs of size $N = 10^4$. (b) The performance of CTGA algorithm of $H = 3$ and $\beta = 23$ and WN algorithm on random regular graphs with $D = 4, K = 3$, and different values of N . The algorithmic results are averaged over 12 instances of random regular graphs for each value of N .

Taking advantage of our model, we build a Cycle-Tree-Guided-Attack (CTGA) algorithm 1. The algorithm is analogous to the sequential importance sampling[28]. However, for larger values of H , the BP equation does not converge, and asynchronous update and simple damping do not seem to alleviate this issue. The reinforcement technique[17, 18] doesn't seem to help improve the performance of the CTGA algorithm. Nonetheless, we disregard the convergence issue and carry out the sampling at each iteration for a specified

number of repeats. In all experiments, to balance calculation time and performance, we set the number of repeats of the BP iteration to 1 and set the damping parameter to about 0.3.

The performance of CTGA has slight dependence on the inverse temperature β and it performs best at intermediate β values (shown in Figure 3(a)). It may be due to the phenomenon that if β is too large, the BP iterations are strongly divergent. Thus, for a given graph, we execute algorithm 1 over a range of inverse temperature β given by the prior and choose the optimal attack set. We also consider the performance on RR graphs with the same degree D and different sizes N (Figure 3(b)). When the scale of a random regular graph is small, the CTGA algorithm may suffer from the low sparsity of the graph. As the increase of graph scale, the average K -core attack density will decrease and converge, and the standard deviation will decrease.

The results of the CTGA are displayed in Table 1 for random regular graphs in comparison with the WN algorithm[26] which was shown to be a state-of-the-art algorithm. The CTGA algorithm outperforms the WN algorithm in all cases, even with relatively low H , and the performance of CTGA can be further enhanced by increasing H at the cost of an increase in computational complexity. Additionally, the results on Erdős–Rényi graphs are shown in Table 2 where the CTGA algorithm with $H = 3$ outperforms the WN algorithm on this random graph ensemble. The performance of this algorithm can be further improved by increasing the time level H , but it will slightly increase the computational complexity.

5 Conclusion

In this paper, we generalize the cycle-tree packing model[30] to the hierarchical version for the minimum K -core attack set problem. We then analyze this hierarchical cycle-tree packing model by replica-symmetric mean field theory of statistical physics. The theoretical ground state energy density on random regular graphs decreases and converges as the number of layers H increases, which gives a glimpse of the potential for algorithmic improvements. The heuristic CTGA algorithm on random regular and Erdős–Rényi graphs outperforms the WN algorithm[26], the state-of-the-art algorithm, and it's prospected that the CTGA algorithm could be further improved by increasing the value of H .

In this paper, we focus on the replica symmetric estimate of the ground state, and the results will be more precise when considering the one-step replica symmetry broken but it requires more complex computations. There are other ways to improve the CTGA algorithm, due to its dependency on β and the non-convergence of the belief propagation equations. It will be interesting to construct the max-sum algorithm[17, 18] which considers the limit $\beta \rightarrow \infty$ and adapt the reinforcement technique[17, 18] which uses the noisy information in updating the max-sum equations to force the system to converge to higher energy, but it still requires much more cautious handling.

D	K	WN	CTGA	ρ_{\min}	RS Cavity method
3	2	0.2503	0.2501	0.25000	0.25000
4	2	0.3378	0.3335	0.33333	0.33333
	3	0.0747	0.0718	0.08293	0.04628
5	2	0.3964	0.3793	0.37837	0.37847
	3	0.1878	0.1877	0.19520	0.16668
	4	0.0281	0.0264	0.03324	0.01311
6	2	0.4444	0.4252	0.42199	0.42262
	3	0.2649	0.2621	0.26742	0.25000
	4	0.1085	0.1075	0.11654	0.07623
	5	0.0138	0.0128	0.01799	0.00572
7	2	0.4836	0.4641	0.45892	0.46001
	3	0.3209	0.3115	0.31719	0.30009
	4	0.1817	0.1801*	0.17742*	0.15005
	5	0.0694	0.0691	0.06973	0.04283
	6	0.0080	0.0075	0.01141	0.00310

Table 1 Performance results of two algorithms: WN[26] and CTGA algorithm, as well as the conjectured optimal results obtained via the RS cavity method in [14] for random regular graphs of degree D . The value of H in CTGA is set to 3 except for the case $D = 7, K = 4$ where it is $H = 4$ (when $D = 7, K = 4$ and $H = 3$, the average cardinality density of attack set is 0.1825, so increasing the value of T will further improve the performance of CTGA). Note that for the case of $K = 2$, the value of T does not affect the performance of CTGA. The algorithmic results are averaged over 12 runs of graph size $N = 10^4$. The values of ρ_{\min} are the theoretical ground state energy densities of the cycle-tree packing model and the values of D, K , and H are the same as the corresponding CTGA.

D	K	WN	CTGA
3	2	0.1394	0.1353
4	2	0.2198	0.2138
	3	0.0357	0.0345
5	2	0.2874	0.2790
	3	0.1019	0.1016
6	2	0.3438	0.3343
	3	0.1645	0.1630
	4	0.0433	0.0419
7	2	0.3907	0.3808
	3	0.2196	0.2180
	4	0.0987	0.0976
	5	0.0083	0.0069

Table 2 Performance results of two algorithms: the WN[26] and the CTGA algorithm for Erdős–Rényi graphs of average degree D . The value of H in the CTGA is set to 3 for all D and K . All algorithmic results are averaged over 12 runs of graph size $N = 10^4$.

The hierarchical cycle-tree packing model offers a fresh perspective on the k -core collapse and an efficient heuristic CTGA algorithm for the minimum K -core attack set problem. The central idea is to represent irreversible K -core pruning dynamics in the graph by static and hierarchical (cycle-)trees. The transformation of a long-range correlated dynamical process into static structural patterns may be fruitful for some optimization problems, such as the generalized K -core percolation problem on directed graphs[31], the directed

feedback vertex (or arc) set problem[20, 32], or the K -core attack by deleting edges[33].

6 Acknowledgments

This work was supported by the National Natural Science Foundation of China (Grant Nos. 11975295, and 12047503), and the Chinese Academy of Sciences (Grant Nos. QYZDJ-SSW-SYS018, and XDPD15). Numerical simulations were carried out at the Tianwen clusters of ITP-CAS.

7 Appendix

7.1 The derivation of the coarse-grained BP equation

We now adopt the standard cavity method of statistical physics[28, 29] to estimate the marginal probability of each vertex. By following the same procedure of ref. [17, 20], the self-consistent belief-propagation (BP) equation can be derived.

Since the nearby constraints $C(A_i, \underline{A}_{\partial i})$ and $C(A_j, \underline{A}_{\partial j})$ share two variables A_i and A_j , the factor graph contains short loops. To deal with this problem, we convert the original graph G to a bipartite graph of factor nodes as shown in Figure 4. The variable nodes represent the pairs of adjacent nodes with composite states (A_i, A_j) for $(i, j) \in E$, while the factor nodes are associated with the vertices i of the original graph G and satisfy the local constraints $C(A_i, \underline{A}_{\partial i})$.

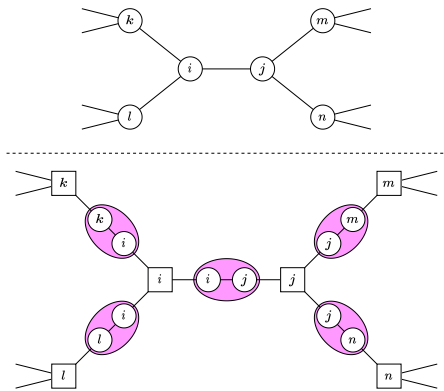


Fig. 4 (top) The part of the original graph G . In this example, $\partial i = \{k, j, l\}$ and $\partial j = \{i, m, n\}$. The cycles represent the vertices of graph G . (down) The bipartite factor graph corresponds to graph G on the top. The link (i, j) is represented by a variable node (shown as an ellipse) and is assigned a composite state (A_i, A_j) . The factor node i (shown as a square) represents a many-body interaction involving node i and its neighbors in graph G . Each variable node (i, j) is connected to exactly two factor nodes i and j .

We denote $q_{i \rightarrow j}(A_i, A_j)$ by the cavity marginal (or belief), the marginal probability of variable (A_i, A_j) in the absence of factor node j . The belief-propagation equation for all directed edges read

$$q_{i \rightarrow j}(A_i, A_j) = \frac{1}{z_{i \rightarrow j}} \sum_{\underline{A}_{\partial i \setminus j}} e^{-\beta \delta_{A_i}} C_i(A_i, \underline{A}_{\partial i}) \prod_{k \in \partial i \setminus j} q_{k \rightarrow i}(A_k, A_i) \quad (16)$$

where $z_{i \rightarrow j}$ is a normalization constant such that $\sum_{A_i, A_j} q_{i \rightarrow j}(A_i, A_j) = 1$, set $\partial i \setminus j$ contains all the neighbors of vertex i except for j , and $\underline{A}_{\partial i} \equiv \{A_k : k \in \partial i\}$. For each directed edge, there are $((d_i + 1)H + 1)((d_j + 1)H + 1)$ states where d_i is the degree of vertex i . Those BP equations can be solved by iteration. Once the fixed points are known, the marginal probability of variable

A_i can be calculated as $q_i(A_i) = \frac{1}{z_i} \sum_{\underline{A}_{\partial i}} e^{-\beta \delta_{A_i}} C_i(A_i, \underline{A}_{\partial i}) \prod_{k \in \partial i} q_{k \rightarrow i}(A_k, A_i)$,

where z_i is a normalization constant ensuring that $\sum_{A_i} q_i(A_i) = 1$. Moreover, the marginal probability of joint variable (A_i, A_j) is given by $q_{ij}(A_i, A_j) = \frac{1}{z_{ij}} q_{i \rightarrow j}(A_i, A_j) q_{j \rightarrow i}(A_j, A_i)$, where z_{ij} is a normalization constant ensuring that $\sum_{A_i, A_j} q_{ij}(A_i, A_j) = 1$. We could evaluate the marginal probability q_i^0 of vertex i being empty, and then the average density (or the average energy density) is expressed as $\rho = \frac{1}{N} \sum_i q_i^0$. The free energy density is given by

$$f = -\frac{1}{\beta N} \sum_i \ln z_i + \frac{1}{\beta N} \sum_{(i,j) \in E} \ln z_{ij} \quad (17)$$

Then the entropy density is simply $s = \beta(\rho - f)$.

By putting the constraint (1) into Equation (16), we notice that there is more compact parametrization for the BP equation. For each $q_{i \rightarrow j}(A_i, A_j)$, among the $((d_i + 1)H + 1)((d_j + 1)H + 1)$ states, there are only $1 + 4H + 3(d_i - 1)(H - 1)$ are distinct. Furthermore, since certain $q_{i \rightarrow j}(A_i, A_j)$ s always appear under the form of particular linear combinations, we can merge them together. Thus, we define the coarse-grained cavity marginal probability by

$$Q_{i \rightarrow j}^0 = \frac{1}{1 + Hd_j} \left[q_{i \rightarrow j}(0, 0) + \sum_{t=1}^H q_{i \rightarrow j}(0, j^t) + \sum_{t=1}^H \sum_{l \in \partial j \setminus i} q_{i \rightarrow j}(0, l^t) \right]; \quad (18a)$$

$$Q_{i \rightarrow j}^{1,1} = \frac{1}{2} \left[q_{i \rightarrow j}(i^1, 0) + q_{i \rightarrow j}(i^1, i^1) + \sum_{k \in \partial i \setminus j} q_{i \rightarrow j}(k^1, 0) + \sum_{k \in \partial i \setminus j} q_{i \rightarrow j}(k^1, i^1) \right]; \quad (18b)$$

$$Q_{i \rightarrow j}^{1,t} = \frac{1}{(t-2)d_j + 2} \left[q_{i \rightarrow j}(i^t, 0) + \sum_{k \in \partial i \setminus j} q_{i \rightarrow j}(k^t, 0) + \sum_{s=1}^{t-1} q_{i \rightarrow j}(i^t, j^s) + \sum_{s=1}^{t-2} \sum_{l \in \partial j \setminus i} q_{i \rightarrow j}(i^t, l^s) + \sum_{s=1}^{t-1} \sum_{k \in \partial i \setminus j} q_{i \rightarrow j}(k^t, j^s) + \sum_{s=1}^{t-2} \sum_{k \in \partial i \setminus j} \sum_{l \in \partial j \setminus i} q_{i \rightarrow j}(k^t, l^s) \right], \quad 2 \leq t \leq H; \quad (18c)$$

$$Q_{i \rightarrow j}^{2,t} = \frac{1}{d_j} \left[q_{i \rightarrow j}(i^t, i^t) + \sum_{l \in \partial j \setminus i} q_{i \rightarrow j}(i^t, l^{t-1}) + \sum_{k \in \partial i \setminus j} q_{i \rightarrow j}(k^t, i^t) + \sum_{k \in \partial i \setminus j} \sum_{l \in \partial j \setminus i} q_{i \rightarrow j}(k^t, l^{t-1}) \right], \quad 2 \leq t \leq H; \quad (18d)$$

$$Q_{i \rightarrow j}^{3,t} = \frac{1}{(H-t)d_j} \sum_{s=t+1}^H \left[q_{i \rightarrow j}(i^t, j^s) + \sum_{l \in \partial j \setminus i} q_{i \rightarrow j}(i^t, l^s) \right], \quad 1 \leq t \leq H-1; \quad (18e)$$

$$Q_{i \rightarrow j}^{4,t} = \frac{1}{d_j} \left[q_{i \rightarrow j}(j^t, j^t) + \sum_{l \in \partial j \setminus i} q_{i \rightarrow j}(j^t, l^t) \right], \quad 1 \leq t \leq H; \quad (18f)$$

$$Q_{i \rightarrow j}^{5,t} = \frac{1}{(H-t+1)d_j - 1} \sum_{k \in \partial i \setminus j} \left[\sum_{s=t+1}^H q_{i \rightarrow j}(k^t, j^s) + \sum_{s=t}^H \sum_{l \in \partial j \setminus i} q_{i \rightarrow j}(k^t, l^s) \right], \quad 1 \leq t \leq H. \quad (18g)$$

By substituting them into the BP equation (16), we obtain the corresponding coarse-grained BP equation (8) shown in the main text.

7.2 BP equation for random regular graphs

For the random regular graphs, we could assume that the cavity probability distributions $Q_{i \rightarrow j}^\sigma$ are the same for all directed edges (i, j) . Then the BP equations are simplified to

$$Q^0 \propto e^{-\beta} \left(Q^0 + \sum_{t=1}^H Q^{1,t} \right)^{D-1}; \quad (19a)$$

$$Q^{1,1} \propto \sum_{n=0}^{K-1} C_{D-1}^n \left(\sum_{t=2}^H Q^{1,t} \right)^n (Q^0 + Q^{4,1})^{D-1-n} + (D-1)Q^{1,1} \\ \times \sum_{n=0}^{K-2} C_{D-2}^n \left(Q^{5,1} + Q^{2,2} + \sum_{t=3}^T Q^{1,t} \right)^n (Q^0 + Q^{4,1})^{D-2-n}; \quad (19b)$$

$$Q^{3,1} \propto \sum_{n=0}^{K-2} C_{D-1}^n \left(\sum_{t=2}^H Q^{1,t} \right)^n (Q^0 + Q^{4,1})^{D-1-n}; \quad (19c)$$

$$Q^{4,1} \propto \sum_{n=0}^{K-2} C_{D-1}^n \left(Q^{5,1} + Q^{2,2} + \sum_{t=3}^H Q^{1,t} \right)^n (Q^0 + Q^{4,1})^{D-1-n}; \quad (19d)$$

$$Q^{5,1} \propto (D-1)Q^{1,1} \sum_{n=0}^{K-3} C_{D-2}^n \left(Q^{5,1} + Q^{2,2} + \sum_{t=3}^H Q^{1,t} \right)^n (Q^0 + Q^{4,1})^{D-2-n}; \quad (19e)$$

$$Q^{1,t} \propto \sum_{n=0}^{K-1} \sum_{m=K-n}^{D-1-n} C_{D-1}^n C_{D-1-n}^m \left(\sum_{s=t+1}^H Q^{1,s} \right)^n (Q^{5,t-1} + Q^{4,t})^m \\ \times \left(Q^0 + \sum_{s=1}^{t-1} Q^{3,s} + \sum_{s=1}^{t-2} Q^{5,s} \right)^{D-1-n-m} + (D-1)Q^{2,t} \\ \times \sum_{n \leq K-2} \sum_{m=K-1-n}^{D-2-n} C_{D-2}^n C_{D-2-n}^m \left(Q^{2,t+1} + \sum_{s=t+2}^H Q^{1,s} + Q^{5,t} \right)^n \\ \times (Q^{5,t-1} + Q^{4,t})^m \left(Q^0 + \sum_{s=1}^{t-1} Q^{3,s} + \sum_{s=1}^{t-2} Q^{5,s} \right)^{D-2-n-m}, \quad 2 \leq t \leq T; \quad (19f)$$

$$\begin{aligned}
Q^{2,t} \propto & \sum_{n=0}^{K-1} \sum_{m=K-1-n}^{D-1-n} C_{D-1}^n C_{D-1-n}^m \left(\sum_{s=t+1}^H Q^{1,s} \right)^n (Q^{5,t-1} + Q^{4,t})^m \\
& \times \left(Q^0 + \sum_{s=1}^{t-1} Q^{3,s} + \sum_{s=1}^{t-2} Q^{5,s} \right)^{D-1-n-m} + (D-1)Q^{2,t} \\
& \times \sum_{n=0}^{K-2} \sum_{m=K-2-n}^{D-2-n} C_{D-2}^n C_{D-2-n}^m \left(Q^{2,t+1} + \sum_{s=t+2}^H Q^{1,s} + Q^{5,t} \right)^n \\
& \times (Q^{5,t-1} + Q^{4,t})^m \left(Q^0 + \sum_{s=1}^{t-1} Q^{3,s} + \sum_{s=1}^{t-2} Q^{5,s} \right)^{D-2-n-m}, \quad 2 \leq t \leq H;
\end{aligned} \tag{19g}$$

$$\begin{aligned}
Q^{3,t} \propto & \sum_{n=0}^{K-2} \sum_{m=K-1-n}^{D-1-n} C_{D-1}^n C_{D-1-n}^m \left(\sum_{s=t+1}^H Q^{1,s} \right)^n (Q^{5,t-1} + Q^{4,t})^m \\
& \left(Q^0 + \sum_{s=1}^{t-1} Q^{3,s} + \sum_{s=1}^{t-2} Q^{5,s} \right)^{D-1-n-m}, \quad 2 \leq t \leq H-1;
\end{aligned} \tag{19h}$$

$$\begin{aligned}
Q^{4,t} \propto & \sum_{n=0}^{K-2} \sum_{m=K-1-n}^{D-1-n} C_{D-1}^n C_{D-1-n}^m \left(Q^{2,t+1} + \sum_{s=t+2}^H Q^{1,s} + Q^{5,t} \right)^n \\
& \times (Q^{5,t-1} + Q^{4,t})^m \left(Q^0 + \sum_{s=1}^{t-1} Q^{3,s} + \sum_{s=1}^{t-2} Q^{5,s} \right)^{D-1-n-m}, \quad 2 \leq t \leq H;
\end{aligned} \tag{19i}$$

$$\begin{aligned}
Q^{5,t} \propto & (D-1)Q^{2,t} \sum_{n=0}^{K-3} \sum_{m=K-2-n}^{D-2-n} C_{D-2}^n C_{D-2-n}^m \left(Q^{2,t+1} + \sum_{s=t+2}^H Q^{1,s} + Q^{5,t} \right)^n \\
& \times (Q^{5,t-1} + Q^{4,t})^m \left(Q^0 + \sum_{s=1}^{t-1} Q^{3,s} + \sum_{s=1}^{t-2} Q^{5,s} \right)^{D-2-n-m}, \quad 2 \leq t \leq H;
\end{aligned} \tag{19j}$$

where $C_D^n \equiv \frac{D!}{n!(D-n)!}$ is the binomial coefficient, and the normalization condition becomes

$$\begin{aligned}
1 = & (1 + DH)Q^0 + 2Q^{1,1} + \sum_{t=2}^H [((t-2)D + 2)Q^{1,t} + DQ^{2,t}] \\
& + \sum_{t=1}^{H-1} (H-t)DQ^{3,t} + \sum_{t=1}^H [DQ^{4,t} + ((H-t+1)D-1)Q^{5,t}].
\end{aligned} \tag{20}$$

A trivial fixed point of Equation (19) is all cavity probability distributions equal to zero. However, we are interested in the non-trivial fixed points of Equation (19) which can be obtained by numerical calculation like the Newton–Raphson method for any given β . After obtaining the non-trivial fixed

point of Equation (19), we can calculate the average density of attack vertices (or the average energy density), the free energy density, and the entropy density of the system. The average energy density is given by

$$\rho = \frac{1}{z_i} e^{-\beta} \left(Q^0 + \sum_{t=1}^H Q^{1,t} \right)^D, \quad (21)$$

where

$$\begin{aligned} z_i = & e^{-\beta} \left(Q^0 + \sum_{t=1}^H Q^{1,t} \right)^D + \sum_{n=0}^{K-1} C_D^n \left(\sum_{t=2}^H Q^{1,t} \right)^n (Q^0 + Q^{4,1})^{D-n} \\ & + DQ^{1,1} \sum_{n=0}^{K-2} C_{D-1}^n \left(Q^{5,1} + Q^{2,2} + \sum_{t=3}^H Q^{1,t} \right)^n (Q^0 + Q^{4,1})^{D-1-n} \\ & + \sum_{t=2}^H \sum_{n=0}^{K-1} \sum_{m=K-n}^{D-n} C_D^n C_{D-n}^m \left(\sum_{s=t+1}^H Q^{1,s} \right)^n (Q^{5,t-1} + Q^{4,t})^m \\ & \times \left(Q^0 + \sum_{s=1}^{t-1} Q^{3,s} + \sum_{s=1}^{t-2} Q^{5,s} \right)^{D-n-m} + \sum_{t=2}^H DQ^{2,t} \\ & \times \sum_{n=0}^{K-2} \sum_{m=K-1-n}^{D-1-n} C_{D-1}^n C_{D-1-n}^m \left(Q^{2,t+1} + \sum_{s=t+2}^H Q^{1,s} + Q^{5,t} \right)^n \\ & \times (Q^{5,t-1} + Q^{4,t})^m \left(Q^0 + \sum_{s=1}^{t-1} Q^{3,s} + \sum_{s=1}^{t-2} Q^{5,s} \right)^{D-1-n-m}. \end{aligned} \quad (22)$$

To obtain the free energy density, we need to calculate another normalization constant, i.e.,

$$\begin{aligned} z_{ij} = & Q^0 Q^0 + 2Q^{1,1} Q^{4,1} + 2Q^0 \sum_{t=1}^H Q^{1,t} + 2 \sum_{t=2}^H Q^{2,t} Q^{4,t} + 2 \sum_{t=2}^H \sum_{s=1}^{t-1} Q^{1,t} Q^{3,s} \\ & + 2 \sum_{t=3}^H \sum_{s=1}^{t-2} Q^{1,t} Q^{5,s} + 2 \sum_{t=1}^{H-1} Q^{2,t+1} Q^{5,t} + \sum_{t=1}^H Q^{5,t} Q^{5,t}. \end{aligned} \quad (23)$$

Thus, the free energy density is given by

$$f = -\frac{1}{\beta} \ln z_i + \frac{D}{2\beta} \ln z_{ij}. \quad (24)$$

Finally, the entropy density is simply $s = \beta(\rho - f)$.

References

- [1] M. Pollak, I. Riess, Application of percolation theory to 2d-3d heisenberg ferromagnets. *physica status solidi (b)* **69**(1), K15–K18 (1975). <https://doi.org/https://doi.org/10.1002/pssb.2220690138>. URL <https://onlinelibrary.wiley.com/doi/abs/10.1002/pssb.2220690138>
- [2] M. Granovetter, Threshold models of collective behavior. *American Journal of Sociology* **83**(6), 1420–1443 (1978). <https://doi.org/10.1086/226707>. URL <https://www.journals.uchicago.edu/doi/abs/10.1086/226707>
- [3] S.B. Seidman, Network structure and minimum degree. *Social Networks* **5**(3), 269–287 (1983). [https://doi.org/10.1016/0378-8733\(83\)90028-x](https://doi.org/10.1016/0378-8733(83)90028-x). URL <https://www.sciencedirect.com/science/article/abs/pii/037887338390028X?via%3Dihub>
- [4] Y.X. Kong, G.Y. Shi, R.J. Wu, Y.C. Zhang, k-core: Theories and applications. *Physics Reports–Review Section of Physics Letters* **832**, 1–32 (2019). <https://doi.org/10.1016/j.physrep.2019.10.004>. URL <https://www.gotolibrary.org/doi/abs/10.1016/j.physrep.2019.10.004>. <https://www.wos.com/doi/abs/10.1016/j.physrep.2019.10.004>. Ju4ka Times Cited:9 Cited References Count:137
- [5] M. Altaf-Ul-Amine, K. Nishikata, T. Korna, T. Miyasato, Y. Shinbo, M. Arifuzzaman, C. Wada, M. Maeda, T. Oshima, H. Mori, S. Kanaya, Prediction of protein functions based on k-cores of protein-protein interaction networks and amino acid sequences. *Genome Informatics* **14**, 498–499 (2003). <https://doi.org/10.11234/gi1990.14.498>
- [6] S. Wuchty, E. Almaas, Peeling the yeast protein network. *PROTEOMICS* **5**(2), 444–449 (2005). <https://doi.org/https://doi.org/10.1002/pmic.200400962>. URL <https://analyticalsciencejournals.onlinelibrary.wiley.com/doi/abs/10.1002/pmic.200400962>
- [7] F. Arese Lucini, G. Del Ferraro, M. Sigman, H.A. Makse, How the brain transitions from conscious to subliminal perception. *Neuroscience* **411**, 280–290 (2019). <https://doi.org/https://doi.org/10.1016/j.neuroscience.2019.03.047>. URL <https://www.sciencedirect.com/science/article/pii/S0306452219302052>
- [8] W.C. Stanford, P.J. Mucha, E. Dayan, A robust core architecture of functional brain networks supports topological resilience and cognitive performance in middle- and old-aged adults. *Proceedings of the National Academy of Sciences* **119**(44), e2203682,119 (2022). <https://doi.org/doi:10.1073/pnas.2203682119>. URL <https://www.pnas.org/doi/abs/10.1073/pnas.2203682119>

- [9] J. Garcia-Algarra, J.M. Pastor, J.M. Iriondo, J. Galeano, Ranking of critical species to preserve the functionality of mutualistic networks using the k-core decomposition. *PeerJ* **5**, e3321 (2017). <https://doi.org/10.7717/peerj.3321>. URL <https://www.ncbi.nlm.nih.gov/pubmed/28533969>. Garcia-Algarra, Javier Pastor, Juan Manuel Iriondo, Jose Maria Galeano, Javier eng 2017/05/24 PeerJ. 2017 May 18;5:e3321. doi: 10.7717/peerj.3321. eCollection 2017.
- [10] M. Kitsak, L.K. Gallos, S. Havlin, F. Liljeros, L. Muchnik, H.E. Stanley, H.A. Makse, Identification of influential spreaders in complex networks. *Nature Physics* **6**(11), 888–893 (2010). <https://doi.org/10.1038/nphys1746>. URL <https://doi.org/10.1038/nphys1746>
- [11] J. Chalupa, P.L. Leath, G.R. Reich, Bootstrap percolation on a bethe lattice. *Journal of Physics C: Solid State Physics* **12**(1), L31–L35 (1979). <https://doi.org/10.1088/0022-3719/12/1/008>. URL <http://dx.doi.org/10.1088/0022-3719/12/1/008>
- [12] D. Reichman, New bounds for contagious sets. *Discrete Mathematics* **312**(10), 1812–1814 (2012). <https://doi.org/https://doi.org/10.1016/j.disc.2012.01.016>. URL <https://www.sciencedirect.com/science/article/pii/S0012365X12000301>
- [13] A. Coja-Oghlan, U. Feige, M. Krivelevich, D. Reichman, *Contagious Sets in Expanders* (Society for Industrial and Applied Mathematics, 2014), pp. 1953–1987. Proceedings. <https://doi.org/doi:10.1137/1.9781611973730.131110.1137/1.9781611973730.131>. URL <https://doi.org/10.1137/1.9781611973730.131>. Doi:10.1137/1.9781611973730.131
- [14] A. Guggiola, G. Semerjian, Minimal contagious sets in random regular graphs. *Journal of Statistical Physics* **158**(2), 300–358 (2015). <https://doi.org/10.1007/s10955-014-1136-2>. URL <https://www.gotolisi.org/WOS/000347875400002>. Ay9mo Times Cited:22 Cited References Count:76
- [15] P.A. Dreyer, F.S. Roberts, Irreversible k-threshold processes: Graph-theoretical threshold models of the spread of disease and of opinion. *Discrete Applied Mathematics* **157**(7), 1615–1627 (2009). <https://doi.org/https://doi.org/10.1016/j.dam.2008.09.012>. URL <https://www.sciencedirect.com/science/article/pii/S0166218X08004393>
- [16] F. Zhang, Y. Zhang, L. Qin, W. Zhang, X. Lin, Finding critical users for social network engagement: The collapsed k-core problem. Proceedings of the AAAI Conference on Artificial Intelligence **31**(1) (2017). <https://doi.org/10.1609/aaai.v31i1.10482>. URL <https://ojs.aaai.org/index.php/AAAI/article/view/10482>

- [17] F. Altarelli, A. Braunstein, L. Dall’Asta, R. Zecchina, Optimizing spread dynamics on graphs by message passing. *Journal of Statistical Mechanics: Theory and Experiment* **2013**(09), P09,011 (2013). <https://doi.org/10.1088/1742-5468/2013/09/p09011>. URL <http://dx.doi.org/10.1088/1742-5468/2013/09/P09011>
- [18] F. Altarelli, A. Braunstein, L. Dall’Asta, R. Zecchina, Large deviations of cascade processes on graphs. *Physical Review E* **87**(6) (2013). <https://doi.org/10.1103/physreve.87.062115>. URL <https://dx.doi.org/10.1103/physreve.87.062115>
- [19] A. Braunstein, L. Dall’Asta, G. Semerjian, L. Zdeborová, Network dismantling. *Proceedings of the National Academy of Sciences* **113**(44), 12,368–12,373 (2016). <https://doi.org/10.1073/pnas.1605083113>. URL <https://dx.doi.org/10.1073/pnas.1605083113>
- [20] H.J. Zhou, A spin glass approach to the directed feedback vertex set problem. *Journal of Statistical Mechanics: Theory and Experiment* **2016**(7), 073,303 (2016). <https://doi.org/10.1088/1742-5468/2016/07/073303>. URL <http://dx.doi.org/10.1088/1742-5468/2016/07/073303>
- [21] J.H. Zhao, H.J. Zhou, Optimal disruption of complex networks. arXiv preprint server (2016). <https://doi.org/Nonearxiv:1605.09257>. URL <https://arxiv.org/abs/1605.09257>
- [22] R.M. Karp, *Reducibility among Combinatorial Problems* (Springer US, Boston, MA, 1972), pp. 85–103. <https://doi.org/10.1007/978-1-4684-2001-2.9>. URL <https://doi.org/10.1007/978-1-4684-2001-2.9>
- [23] S. Bau, N.C. Wormald, S. Zhou, Decycling numbers of random regular graphs. *Random Structures & Algorithms* **21**(3-4), 397–413 (2002). <https://doi.org/https://doi.org/10.1002/rsa.10069>. URL <https://onlinelibrary.wiley.com/doi/abs/10.1002/rsa.10069>
- [24] H.J. Zhou, Spin glass approach to the feedback vertex set problem. *The European Physical Journal B* **86**(11), 455 (2013). <https://doi.org/10.1140/epjb/e2013-40690-1>. URL <https://doi.org/10.1140/epjb/e2013-40690-1>
- [25] L. Zdeborová, P. Zhang, H.J. Zhou, Fast and simple decycling and dismantling of networks. *Scientific Reports* **6**(1), 37,954 (2016). <https://doi.org/10.1038/srep37954>. URL <https://doi.org/10.1038/srep37954>
- [26] C. Schmidt, H.D. Pfister, L. Zdeborova, Minimal sets to destroy the k-core in random networks. *Phys Rev E* **99**(2-1), 022,310 (2019). <https://doi.org/10.1103/PhysRevE.99.022310>. URL <https://www.ncbi.nlm.nih.gov/pubmed/30934241>. Schmidt, Christian Pfister, Henry D Zdeborova,

- Lenka eng Phys Rev E. 2019 Feb;99(2-1):022310. doi: 10.1103/Phys-RevE.99.022310.
- [27] S. Pei, X. Teng, J. Shaman, F. Morone, H.A. Makse, Efficient collective influence maximization in cascading processes with first-order transitions. *Scientific Reports* **7**(1), 45,240 (2017). <https://doi.org/10.1038/srep45240>. URL <https://doi.org/10.1038/srep45240>
- [28] M. Mézard, A. Montanari, *Information, Physics, and Computation* (Oxford University Press, 2009). <https://doi.org/10.1093/acprof:oso/9780198570837.001.0001>
- [29] H. Zhou, *Spin Glass and Message Passing* (Science Press, Beijing, 2015)
- [30] H.J. Zhou, Cycle-tree guided attack of random k-core: Spin glass model and efficient message-passing algorithm. *Science China Physics, Mechanics & Astronomy* **65**(3), 230,511 (2022). <https://doi.org/10.1007/s11433-021-1845-6>. URL <https://doi.org/10.1007/s11433-021-1845-6>
- [31] J.H. Zhao, Generalized k -core pruning process on directed networks. *Journal of Statistical Mechanics: Theory and Experiment* **2017**, 063,407 (2017). <https://doi.org/10.1088/1742-5468/aa71e0>
- [32] Y.Z. Xu, H.J. Zhou, Optimal segmentation of directed graph and the minimum number of feedback arcs. *Journal of Statistical Physics* **169**(1), 187–202 (2017). <https://doi.org/10.1007/s10955-017-1860-5>. URL <https://dx.doi.org/10.1007/s10955-017-1860-5>
- [33] B. Zhou, Y. Lv, J. Wang, J. Zhang, Q. Xuan. Coreattack: Breaking up the core structure of graphs (2021). URL <https://ui.adsabs.harvard.edu/abs/2021arXiv211115276Z>